Asian Journal of Chemistry; Vol. 33, No. 9 (2021), 2038-2042

ASIAN JOURNAL OF CHEMISTRY

https://doi.org/10.14233/ajchem.2021.23255

Silver Doped TiO_2 Photocatalyst for Disinfection of *E. coli* and Microplastic Pollutant Degradation in Water

M.F. HARIS[1], A.M. DIDIT[1], M. IBADURROHMAN[1], SETIADI[1] and SLAMET[1,*]

Departement of Chemical Engineering, Faculty of Engineering, Universitas Indonesia, Depok, Indonesia

*Corresponding author: Fax: +62 21 7863515; Tel: +62 21 7863516; E-mail: slamet@che.ui.ac.id

Received: 20 April 2021; *Accepted*: 11 June 2021; *Published online*: 20 August 2021; AJC-20461

Present study report the synthesis of Ag/TiO_2 catalyst to study its ability to disinfect the pathogenic microorganisms and degrade into micropollutants in water. The Ag/TiO_2 was synthesized by photoassisted deposition (PAD) method. The ratio of silver dopant varied (1%, 3% and 5%) to the total weight of the composite. The SEM-EDX, UV-Vis DRS and XRD techniques were used to characterize and determine the influence of silver dopant on the TiO_2 structure. In this study, the microorganism used was *Escherichia coli* and the microplastic used was polyethylene. During the photocatalytic process under ultraviolet light irradiation, a magnetic stirrer was used at 2000 rpm. The performance of photocatalyst in *E. coli* disinfection and microplastic degradation improved by the addition of silver dopant. The 3% silver dopant has optimum performance with 79% of microbial disinfection within 2 h and 81% microplastic degradation within 4 h.

Keywords: Microplastics, Microorganism, Silver dopant, Photocatalyst, Water.

INTRODUCTION

A study by the State University of New York at Fredonia examined the issue of pollutants present in the latest bottled water in 2018. The trial tested 259 bottles of 11 drinking water brands sold in eight countries. It was found that 93% of water contained microplastics [1]. A sample taken from Indonesia contains an average of 382 microplastic particles per liter, ranging in size from 6.5 to over 100 μ [1]. It is well known that bottled drinking water samples extracted from local products contain as many as 4,713 microplastic particles per liter. Non-local drinking water samples can contain up to 10,390 particles per liter of microplastics containing polypropylene, nylon, polystyrene and polyethylene types [1]. The test brought back bottled water products under the same brand in the laboratory of the Faculty of Mathematics and Science, University of Indonesia and found that the microplastic particle size was 11 to 247 μ [2]. It is well known that the microplastic carcinogenicity of particles contained in drinking water can cause cancer [3]. The physical presence of microplastics as pollutants can also trigger the clotting of the digestive tract. It is believed that if the content of microplastics is less than 150 μm [4], they can also moved to the human body. Therefore, it should be emphasized that drinking water purification technology can not only separate the particle size based on microplastics but also decompose into harmless compounds.

The most important component in a water purification unit is a technology that can be used to disinfect pathogenic microorganisms and degrade other pollutants. Plasma ion technology has been widely used as the main component of ion generators, which can generate OH radicals for water purification [5]. However, plasma technology also has a sufficiently high risk related to work safety when it is applied [5]. Therefore, purification technology using photocatalytic nanocomposite materials has been proven as a promising technique for purification and treatment of various kinds of wastewater [6]. Various studies reported [7,8] that combination of several materials into composite materials can lead in the formation of an effective purification unit. Previous studies [9] have shown that TiO_2 nanoparticles compiled with plastic polyethylene particles (1% by weight) exhibit 86% microplastic degradation activity under UV irradiation, but the required high irradiation time of 300 h. To improve the photocatalytic ability, the photocatalyst can be combined with a metal dopant. This increase

is related to the efficiency and ability of the core dopant to trap charge carriers (electron trapping) and reduce the recombination rate between e^- and h^+. The researchers chose metallic silver as the dopant because it has been shown to reduce the bandgap energy, so it can work under visible light and can be used as an electron trapping agent, thereby limiting recombination rate so that electrons can be absorbed. It is easier to excite and improve the photocatalytic activity of TiO_2 [10]. In addition to support the performance of TiO_2 to degrade organic compounds, metallic silver also has the advantage of being an antibacterial agent [11].

In this study, polyethylene microplastics were chosen as samples because they have a wide range of applications in various needs of industry and households [12]. The Ag/TiO_2 was synthesized by photo-assisted deposition (PAD) method, where $AgNO_3$ precursor was added to the TiO_2 P25 slurry, which was then placed in a photoreactor for 6 h. Characterization *viz*. SEM-EDX (scanning electron microscope with energy dispersive X-ray spectroscopy), XRD (X-ray diffraction) and UV-Vis-DRS (UV-vis diffuse reflec-tance spectroscopy) were performed to provide information about the difference between TiO_2 and Ag/TiO_2. Then, ability of Ag/TiO_2 to degrade polyethylene microplastics in water was tested under ultraviolet radiation.

EXPERIMENTAL

Catalyst preparation: The synthesis of Ag/TiO_2 nanocomposite was carried out by using the photo-assisted deposition (PAD) method [13]. In the first step, a TiO_2 slurry was prepared by adding 2 g of TiO_2 in 270 mL distilled water followed by the addition of nitric acid to keep the pH of the slurry to 3 and then placed the slurry in an ultrasonic instrument for 30 min. In the next step, added 0.047 g $AgNO_3$ to the slurry followed by the addition of 1% dopant to Ag/TiO_2 based on the mass of TiO_2 initially used. Stirring was continued for 0.5 h followed by the addition of 30 mL methanol. Finally, the slurry was inserted into the photoreactor under stirring and irradiated for 6 h. The slurry was then centrifuged twice for 30 min at 4000 rpm to separate and the pH of the composite was increased to 6. Finally, the sample was dried at 150 ºC and then calcined at 300 ºC for 1 h.

Characterization: The SEM-EDX characterization of the catalyst was performed to observe the pattern or surface structure of the synthesized Ag/TiO_2 catalyst and observed the percentage of Ag element loading on Ag/TiO_2. The UV-Vis DRS characterization aims to determine the energy gap value of the TiO_2 photocatalyst composite material which has been supported by silver metal. The XRD characterization was done to determine the crystal size and characteristics of the catalyst doped with silver metal.

Analysis of disinfection: The total plate count (TPC) method was used to analyze the disinfection performance of microorganisms modeled on *Escherichia coli*. This method count the colonies of *Escherichia coli* after UV irradiation and photocatalysis. Added 1 mL of *E. coli* in a beaker containing 20 mL distilled water and 20 mg of composite material. The solution was stirred thoroughly and irradiated with UV light in the photoreactor for 2 h. After every 0.5 h, 1 mL sample was pipetted out and diluted with 10 mL of aqueous solution buffered peptone . The dilution factor was 5 times. Then, pour 1 mL diluted sample into a petri dish and filled it with place count agar (PCA) solution. After the PCA solidifies, the petri dish was incubated at 37 ºC for 24 h. The disinfection percentage of the nanocomposite was calculated by using eqn. 1:

$$\text{Disinfection } (\%) = \frac{C_o - C}{C_o} \times 100 \quad (1)$$

where C_o and C are the concentration of *E. coli* in CFU/mL which can be calculated from eqn. 2.

$$C = d \times \frac{N}{V} \quad (2)$$

where N is the total *E. coli* colonies in the plate count agar, d is the dilution factor and V is the volume of sample.

Microplastic degradation test: The microplastic degradation test was performed by adding microplastics made of 100-150 µm polyethylene scrub to distilled water. About 100 mL of aqueous solution and 50 mg of microplastics were added to the beaker followed by the addition of 50 mg of catalyst was added to the solution and the solution was continuously stirred. The degradation test was carried out at room temperature with ultraviolet radiation. The same amount of initial plastic contaminants were analyzed at 1, 2, 3 and 4 h and then filtered the solution using Whatman filter paper 41 in order to filter the undissolved microplastics in the solution. After that the filter paper and microplastics were dried at 100 ºC for 1 h in an oven.

RESULTS AND DISCUSSION

SEM-EDX analysis: The prepared catalyst was characterized by SEM-EDX, the pattern or surface structure of Ag/TiO_2 catalyst was observed and compared with TiO_2 P25. The results of the SEM characterization can be seen in Fig. 1.

Fig. 1 shows the 10,000 times magnification of TiO_2 and Ag/TiO_2 catalysts. It can be seen that the Ag/TiO_2 catalyst formed small agglomerates. The formation of these agglomerates is the result of heat treatment that occurs during the catalyst synthesis process. Using SEM microscope, the silver metal is not very obvious, this is because some metals synthesized by the photo-assisted deposition (PAD) method will have a smaller size (nanometer), which is relatively invisible under the microscope magnification [14]. Table-1 showed the EDX result of silver metal loading was sufficient in the PAD synthesis process. This shows that the method used for the synthesis is appropriate and produces good results.

TABLE-1
PERCENTAGE OF EACH ELEMENT ON THE CATALYST FROM EDX CHARACTERIZATION

Element	1% Ag/TiO_2	3% Ag/TiO_2	5% Ag/TiO_2
Ti	60.81	43.15	59.68
O	38.08	54.14	35.72
Ag	1.11	2.71	4.60

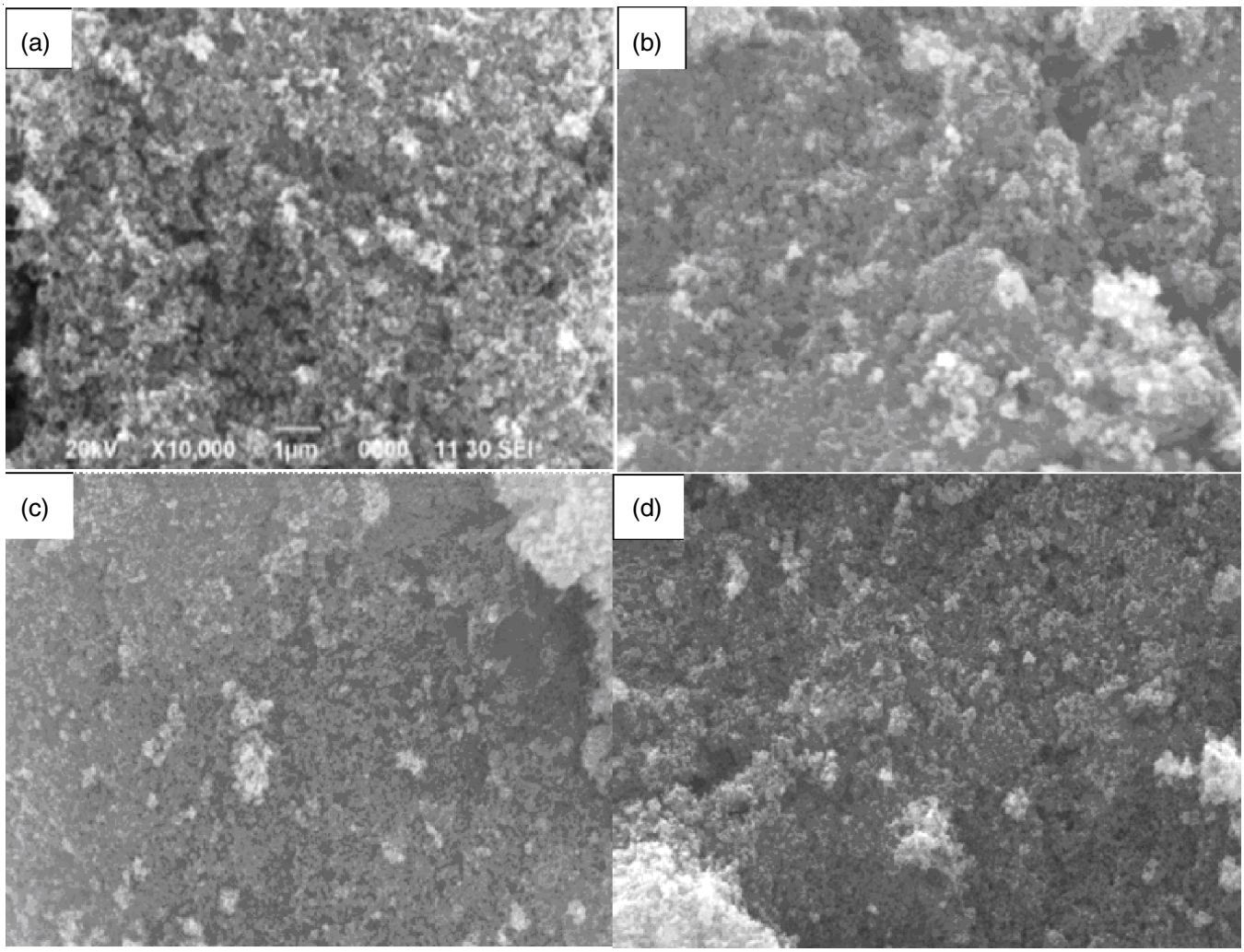

Fig. 1. SEM result on (a) TiO_2, (b) 1% Ag/TiO_2, (c) 3% Ag/TiO_2 and (d) 5% Ag/TiO_2

UV-visible analysis: The gap value of doped composite was compared with the TiO_2 P25 composite to determine the effect of silver metal dopant on the photon absorbance ability of the composite. The results of the characterization of Ag/TiO_2 were compared with the TiO_2 P25 catalyst, which is known to have good responsiveness to UV rays with a wavelength of < 380 nm [15]. Fig. 2 shows the absorbance value of Ag/TiO_2 catalyst with variations in the metal loading of 1, 3 and 5 wt.%.

The value of the energy bandgap for each catalyst was calculated using the Kubelka-Munk equation. By plotting between F(R) against hν and extrapolating in its linear region, the hν value in F(R) can be determined. And F(R) = 0, which is the energy value in the gap of the absorbing species. After extrapolating at F(R) = 0, then on the *x*-axis, the value of the catalyst energy gap band is obtained [16,17]. The energy gap band values for each catalyst are shown in Table-2.

XRD Characterization: XRD patterns of pure TiO_2 and 5% Ag/TiO_2 are shown in Fig. 3. The 2θ values of 25.3º, 37.8º and 48.0º correspond to the anatase phase. Similarly, peaks at 2θ values of 27.4º, 36.1º and 41.2º rutile phase of TiO_2. However, no diffractions peaks in the patterns of silver doped samples were observed. This is probably caused by the silver particle size on TiO_2 which is very small, thus results in the high dispersion

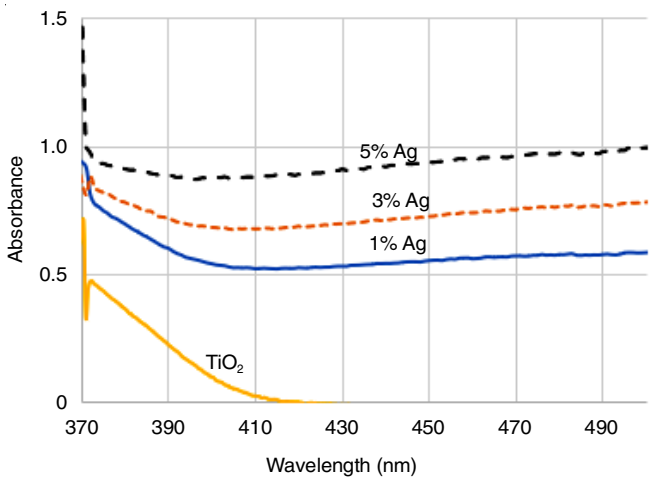

Fig. 2. Absorbance results of the TiO_2 and Ag/TiO_2

TABLE-2
BAND GAP ENERGY CALCULATION

Catalysts	Band gap energy (eV)	Wavelength (nm)
TiO_2 Evonik P25 [15]	3.10	399
1% Ag/TiO_2	3.02	411
3% Ag/TiO_2	2.85	435
5% Ag/TiO_2	2.70	459

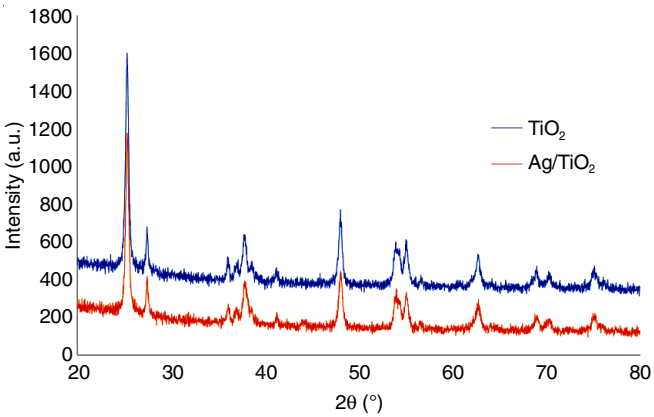

Fig. 3. XRD result of TiO_2 and 5% Ag/TiO_2 catalyst

of dopant species because of the PAD synthetic method [13,14]. The crystalline size and TiO_2 phase percentage in each composite are shown in Table-2.

The anatase crystals on the TiO_2 catalyst are the most active in the photocatalytic process. The more anatase crystals in the catalyst, the better effectiveness of the photocatalytic performance. However, the presence of rutile crystals also exerts the great significance, which indicates that there are no impurities in the catalyst and is more crystalline. The crystal size can be determined by the Scherrer equation and the crystal composition are shown in Table-3.

TABLE-3
CRYSTAL COMPOSITION AND SIZE FROM X-RAY DIFFRACTION

Catalyst	Mass (%)		Crystal size (nm)	
	Anatase	Rutile	Anatase	Rutile
TiO_2 P25	69.97	30.03	21	29
5% Ag/TiO_2	69.14	30.86	20	32

Microorganism disinfection analysis: Fig. 4 displays the results of the photocatalytic disinfection of *E. coli* by TiO_2 and Ag/TiO_2 and without any photocatalyst under UV irradiation. The condition without catalyst and UV irradiation is shown as the control samples. Without catalyst and UV irradiation, the amount of *E. coli* proliferates with time.

Fig. 5 shows that 3% Ag/TiO_2 performs best in *E. coli* disinfection, reaching almost 80% within 2 h under UV irradiation, followed by 1% Ag/TiO_2 and 5% Ag/TiO_2. Among other

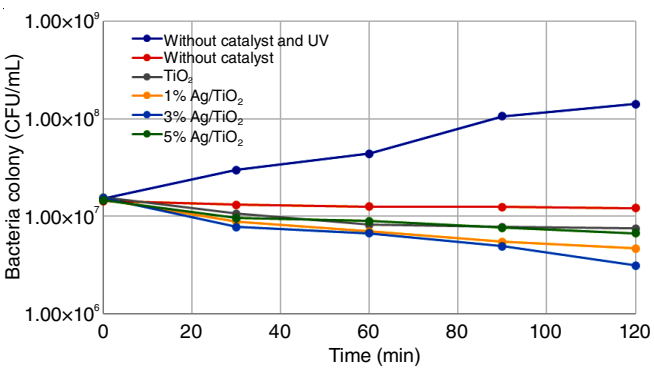

Fig. 4. *E. coli* colony (logarithmic scale) *vs.* time of reaction

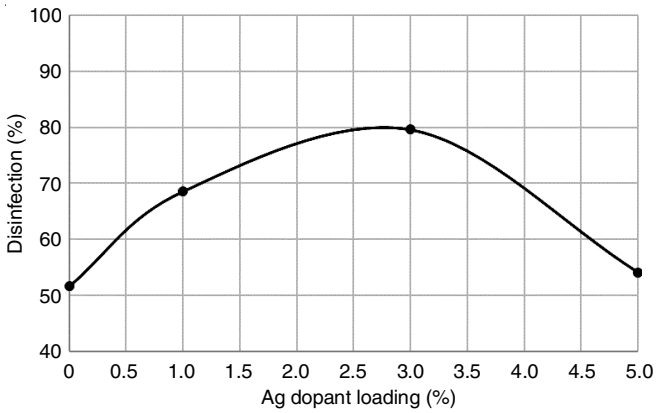

Fig. 5. Disinfection percentage to Ag loading after 2 h irradiation

Ag/TiO_2 samples, 5% Ag/TiO_2 composite showed the lowest disinfection percentage. This indicates that the bactericidal ability does not always increase with the increase in the amount of Ag loaded on TiO_2. This phenomenon may be caused by too much Ag deposited on TiO_2 and covering the active sites of TiO_2, which affects the poor absorption of photons. Therefore, 3% Ag/TiO_2 has the best Ag loading in the disinfection of *E. coli*.

Mechanism: The disinfection of *E. coli* is influenced by TiO_2 catalyst, which is caused by a redox reaction in the bacterial cell membrane that occurs from the presence of hydroxyl radicals and O^{2-} generated after TiO_2 is activated by UV light. Due to the light excitation on the surface of TiO_2 catalyst, the hydroxyl groups and O^{2-} radicals are formed through holes and electrons. Hydroxyl and O^{2-} free radicals attack the outer membrane of *E. coli*, causing the cell membrane to rupture and cause lysis [18]. The destruction of this membrane provides an entry point for hydroxyl and O^{2-} radicals, so they can destroy the contents of the cell. On the other hand, adding Ag metal dopant also has the effect of disinfecting *E. coli*. The Ag metal reacts with water to form Ag^+ and interacts with the SH (retinol) group in the bacteria and then kills the bacteria [19]. Therefore, due to the role of the Ag dopant as an electron trapping agent and a disinfectant, the performance of the catalyst will be improved.

Microplastic degradation analysis: Fig. 6 shows the performance of microplastic degradation using pure TiO_2, Ag/TiO_2 and no catalyst. The results show that the catalyst can degrade the microplastic compounds in water under ultraviolet radiation and the 3% Ag/TiO_2 catalyst has the best degradation ability for 4 h of radiation, with a mass of microplastic remaining after the degradation process is 9.5 mg or 81% of mass degradation percentage, whereas the analysis without a catalyst showed no change in the microplastic mass. This indicates that the degradation process of microplastics under ultraviolet light is affected by the presence of photocatalysts and will not occur without catalysts under ultraviolet light.

Mechanism: The presence of photocatalyst in water under UV irradiation will produce $OH^{\bullet}$, which is a great oxidizing agent which in turn reduce the microplastic pollutant. The overall reaction mechanism of the microplastic degradation by TiO_2 $OH^{\bullet}$ can be explained in eqns. 1-6 [12,20]:

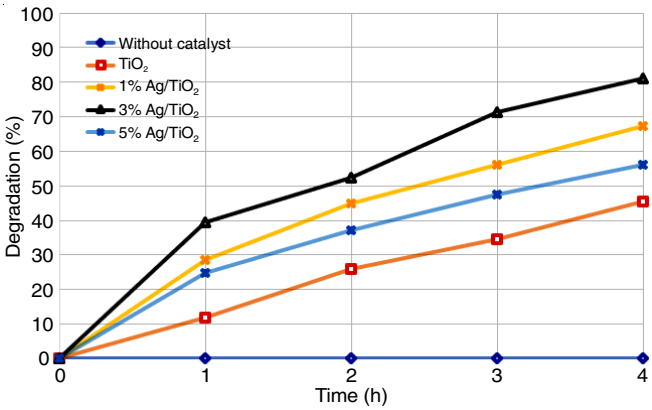

Fig. 6. Percentage of microplastic degradation performance

$$(–CH_2–CH_2–)_n + {}^{\bullet}OH^- \longrightarrow (–CH_2–{}^{\bullet}CH–)_n + H_2O \quad (1)$$

$$(–CH_2–{}^{\bullet}CH–)_n + O_2 \longrightarrow (–CH_2–HCOO^{\bullet}–CH_2–)_n \quad (2)$$

$$(–CH_2–HCOO^{\bullet}–CH_2–)_n + (–CH_2–CH_2–)_n \longrightarrow (–CH_2–HCOOH–CH_2–) + (–CH_2–{}^{\bullet}CH)_n \quad (3)$$

$$(–CH_2–HCOOH–CH_2–)_n \rightarrow (–CH_2–HCO^{\bullet}–CH_2–)_n + {}^{\bullet}OH^- \quad (4)$$

$$(–CH_2–HCO^{\bullet}–CH_2–)_n \longrightarrow \text{Carbonyl groups} \quad (5)$$

$$(–CH_2–HCO) + (–CH_2–COOH) + (CH_2–CO–CH_2–) \longrightarrow CO_2 + H_2O \quad (6)$$

Conclusion

Silver doped TiO_2 exhibited better performance in *E. coli* disinfection and microplastic degradation tests in water bottled samples. The 3 wt.% silver doped on TiO_2 showed optimimum antibacterial activity could disinfect 79.61% of *E. coli* within 2 h UV irradiation, which was higher than 51.6% of pure TiO_2. The microplastic degradation test showed similar results, where 3 %wt. of silver doped on TiO_2 had a higher percentage of degradation, with a percentage of mass degradation of 81%.

ACKNOWLEDGEMENTS

The authors express their gratitude to Ristekdikti PDUPT's grant, contract number NKB-2864/UN2.RST/HKP.05.00/2020, for this study.

CONFLICT OF INTEREST

The authors declare that there is no conflict of interests regarding the publication of this article.

REFERENCES

1. S.A. Mason, V.G. Welch and J. Neratko, *Front. Chem.*, **6**, 407 (2018); https://doi.org/10.3389/fchem.2018.00407
2. C. Tyree, Microplastics, The Most Widespread and Persistent Hazards of Plastic, Toxics Link, Factsheet No. 56, April (2018).
3. V. Benno Meyer-Rochow, J. Valérie Gross, F. Steffany, D. Zeuss and T.C. Erren, *Environ. Res.*, **142**, 575 (2015); https://doi.org/10.1016/j.envres.2015.08.015
4. A. Lusher, In FAO Fisheries and Aquaculture Technical Paper (FAO) eng no. 615 (2017).
5. J.E. Foster, *Phys. Plasmas*, **24**, 055501 (2017); https://doi.org/10.1063/1.4977921
6. J.C. Yu, J. Yu, W. Ho and L. Zhang, *Chem. Commun.*, **19**, 1942 (2001); https://doi.org/10.1039/B105471F
7. M.R. Berber, *J. Chem.*, **2020**, 7608423 (2020); https://doi.org/10.1155/2020/7608423
8. X. Wang, L. Chen, L. Wang, Q. Fan, D. Pan, J. Li, F. Chi, Y. Xie, S. Yu, C. Xiao, F. Luo, J. Wang, X. Wang, C. Chen, W. Wu, W. Shi, S. Wang and X. Wang, *Sci. China Chem.*, **62**, 933 (2019); https://doi.org/10.1007/s11426-019-9492-4
9. X. Zhao, Z. Li, Y. Chen, L. Shi and Y. Zhu, *J. Mol. Catal. Chem.*, **268**, 101 (2007); https://doi.org/10.1016/j.molcata.2006.12.012
10. P.V. Laxma Reddy, B. Kavitha, P.A. Kumar Reddy and K.-H. Kim, *Environ. Res.*, **154**, 296 (2017); https://doi.org/10.1016/j.envres.2017.01.018
11. K. Gupta, R.P. Singh, A. Pandey and A. Pandey, *Beilstein J. Nanotechnol.*, **4**, 345 (2013); https://doi.org/10.3762/bjnano.4.40
12. S.T. Tofa, Ph.D. Dissertation, KTH Royal Institute of Technology: Sweden (2018).
13. S. Somasundaram, Ph.D. Dissertation, Novel Approaches to Photo-assisted Deposition of Semiconductors and Nanocomposite Materials, The University of Texas: Arlington (2006).
14. Z. Sarteep, A.E. Pirbazari and M.A. Aroon, *J. Water Environ. Nanotechnol.*, **1**, 135 (2016); https://doi.org/10.7508/JWENT.2016.02.007
15. C.H. Lee, S.H. Park, W. Chung, J.Y. Kim and S.H. Kim, *Colloids Surf. A Physicochem. Eng. Asp.*, **384**, 318 (2011); https://doi.org/10.1016/j.colsurfa.2011.04.010
16. Ratnawati, Enjarli, and Slamet. In Proceedings of 3rd International Symposium on Applied Chemistry (ISAC), Indonesia, pp. 1-8 (2017).
17. R. Mohamed, I. Mkhalid, S. Al-Thabaiti and M. Mokhtar, *J. Nanosci. Nanotechnol.*, **13**, 4975 (2013); https://doi.org/10.1166/jnn.2013.7602
18. J. Blanco-Galvez, P. Fernández-Ibáñez and S. Malato-Rodríguez, *J. Sol. Energy Eng.*, **129**, 4 (2007); https://doi.org/10.1115/1.2390948
19. R.D. Sun, A. Nakajima, T. Watanabe and K. Hashimoto, *J. Photochem. Photobiol. Chem.*, **154**, 203 (2003); https://doi.org/10.1016/S1010-6030(02)00322-2
20. B. Xin, P. Wang, D. Ding, J. Liu, Z. Ren and H. Fu, *Appl. Surf. Sci.*, **254**, 2569 (2008); https://doi.org/10.1016/j.apsusc.2007.09.002